



Influence of Donnan and dielectric exclusion on ion sorption in sulfonated polysulfones

Sean M. Bannon, Geoffrey M. Geise*

Department of Chemical Engineering, University of Virginia, 385 McCormick Road, Charlottesville, VA, 22903, United States

ARTICLE INFO

Keywords:

Ion exchange membranes
Donnan–Manning model
Dielectric exclusion
Ion sorption
Desalination

ABSTRACT

The Donnan–Manning model accurately describes the thermodynamic properties (e.g., ion sorption) of many charged polymers equilibrated with aqueous electrolytes, such as the commercial ion exchange membranes CR61 and Nafion. It less accurately describes the ion sorption properties of sulfonated polysulfone, which is a promising desalination membrane polymer. One possible explanation is that other ionic interactions that are not included in the Donnan–Manning model, e.g., dielectric exclusion (or ion solvation effects) that can be described via the Born model, may have a significant influence on ion sorption in sulfonated polysulfones. We developed a model to account for the influence of both Donnan–Manning and dielectric exclusion factors on ion sorption properties and applied it to sulfonated polysulfones and Nafion. This Donnan–Manning–Born model described the ion sorption properties of sulfonated polysulfones more accurately than the Donnan–Manning model alone. The Donnan–Manning–Born model also predicted ion sorption properties in Nafion with improved accuracy relative to Donnan–Manning predictions, but the improvement was less significant than in the sulfonated polysulfone case. These results provide an approach for quantifying the influence of dielectric exclusion on ion sorption in charged polymers and could be particularly important for materials where dielectric exclusion is relevant.

1. Introduction

Polymers are promising membrane separation materials that are used in desalination processes that separate salt and water to address global water shortage issues [1–4]. To achieve a given desalination separation via a polymer membrane, salt (i.e., ions) and water must transport through the polymer at different rates [4,5]. Transport of ions and water through a dense polymer can be described by a combination of thermodynamic (i.e., sorption) and kinetic (i.e., diffusion) factors [6–8]. Understanding how polymer structure influences transport properties, through either kinetic or thermodynamic interactions between polymer and water/salt, is needed to inform strategies for engineering polymers with favorable desalination properties.

Charged polymers (i.e., polymers with fixed, ionizable chemical functionality tethered to the polymer backbone) are promising materials for desalination applications due, in part, to their fouling resistance [9, 10], chlorine tolerance [11–13], and ability to reject salt, i.e., mobile ions [2,14–16]. Often, this mobile ion rejection in charged polymers is discussed, to a first approximation, in terms of Donnan exclusion

[17–20]. Donnan exclusion describes how polymers with fixed charges contain a higher concentration of counter-ions (which have the opposite sign as the polymer fixed charges) in the polymer matrix compared to the concentration of co-ions (which have the same sign as the polymer fixed charges) [21,22]. Donnan exclusion is modeled by combining the conditions of electrochemical equilibrium between the polymer and external solution and electroneutrality [20,21], and in principle, the Donnan model could be used in a predictive manner to quantify the ion sorption properties of charged polymers equilibrated with electrolytes [20,23–25].

Critical to the use of the classic Donnan model to predict ion sorption properties of charged polymers is knowledge of the mean ionic activity coefficients in the polymer [17,21], which cannot be measured independently of the polymer ion sorption properties [20,23–27]. In the past, researchers have circumvented this issue by using the ideal Donnan model, where the mean ionic activity coefficient in the polymer is set equal to that in solution (or, where the ratio of the mean ionic activity coefficients in the polymer and solution is set equal to a constant) [16, 20,24,28]. However, the ideal Donnan model does not accurately

* Corresponding author.

E-mail address: geise@virginia.edu (G.M. Geise).

describe the ion sorption properties of many materials, and this discrepancy has led to significant efforts to reconcile the ideal Donnan model and experimentally obtained ion sorption properties [16,20,24].

Recently, the combination of the classic Donnan model and the Manning counter-ion condensation model (the so-called Donnan – Manning model) has advanced efforts to model ion sorption in charged polymers [23,26,27,29,30]. The Donnan – Manning model completes the ideal Donnan model by incorporating the differences between the mean ionic activity coefficients for both the solution and polymer phases [26,29]. The mean ionic activity coefficients can be quantitatively calculated in the polymer phase using the Manning counter-ion condensation model and in the solution phase using a suitable model, e.g., the commonly used Pitzer model [31–34]. While the Donnan – Manning model does not describe the influence of specific ion effects on ion sorption (i.e., does not describe differences in ion sorption properties for polymers equilibrated with different electrolytes of the same valence [26,27,35,36]), it effectively describes the sodium chloride sorption properties of some commercially available charged polymers such as CR61, sulfonated-polystyrene [23] and Nafion, a perfluorinated sulfonated polymer membrane [27] (Fig. 1A).

The Donnan – Manning model does not predict effectively the ion sorption properties of all polymers [29]. For example, the Donnan – Manning model less effectively describes the ion sorption properties of sulfonated polysulfone [11,37–44] (Fig. 1B) compared to CR61 or Nafion (Fig. 1A). The over-prediction of ion sorption in sulfonated polysulfone by the Donnan – Manning model is likely because the Manning model under-predicts the mean ionic activity coefficients for these materials [37].

The observation that the Donnan – Manning model over-predicts ion sorption in sulfonated polysulfone may be related to suggestions that the model most accurately describes ion sorption in high water content polymers (i.e., materials with water volume fractions larger than 0.4) [29]. From a desalination perspective, the most promising sulfonated polysulfone materials have degrees of disulfonation that result in water volume fractions that are less than 0.4 [11,45] and, as a result, are examples of low water content polymers. The observed breakdown of the Donnan – Manning model for low water content polymers may be due to additional ion exclusion as a result of ion solvation effects [46] that are not captured by the Donnan – Manning model and that may become more significant as polymer water content decreases.

These ion solvation effects (and their influence on ion sorption) are sometimes referred to as dielectric exclusion [46–53]. In the simplest case, dielectric exclusion can be described in terms of electrostatic forces using the Born model [53,54], where both the membrane and external

solution phases are taken as homogeneous dielectric media [46,48,55]. If the dielectric constants of the membrane and the solution are different, as is often the case [55], then there is an excess solvation energy associated with the movement of an ion from the solution into the polymer. If this excess solvation energy is positive, as is generally the case for desalination relevant materials [46,55,56], it represents a barrier for the ion sorption process, and mobile ions are excluded from partitioning into the polymer [48]. This excess solvation energy effectively describes how the interactions between ions and their induced polarization charges influence ion sorption processes. Therefore, similar to how the Manning model describes the influence of ion-fixed charge interactions on ion sorption, dielectric exclusion (through the Born model) describes the influence of ion-induced polarization charge interactions on ion sorption.

The dielectric constant of the hydrated polymer is the relevant polymer property that influences ion sorption via the Born model, and the magnitude of dielectric exclusion increases as the dielectric constant decreases [55]. The hydrated polymer dielectric constant depends, to a first approximation, on polymer water content, and low water volume fraction polymers generally have lower dielectric constants than high water volume fraction polymers [46,48,55–57]. Therefore, it is possible that the Donnan – Manning model fails to quantitatively describe ion sorption in low water volume fraction polymers because dielectric exclusion may be more significant in these low dielectric constant materials compared to higher water content materials where the assumptions in the Donnan – Manning model are more appropriate.

This idea suggests a modeling approach where Donnan – Manning and dielectric exclusion effects are combined. Modeling that combines Donnan and dielectric exclusion has been reported [47,58,59]. For example, the peNRTL model proposed by Yu et al. combines Donnan – Manning and dielectric exclusion (among other interactions) and accurately described ion partitioning in a series of sulfonated polymers using few adjustable parameters [60,61]. However, a single predictive model that accounts for Donnan exclusion, the ion-polymer interactions described by the Manning model, and the ion solvation effects described by dielectric exclusion could be useful for describing ion sorption in low water content charged polymers.

Here, we present a mathematical framework to describe the influence of both Donnan – Manning exclusion and dielectric exclusion on the ion sorption properties of hydrated charged polymers. We then compare ion sorption properties, calculated using this approach, to ion sorption properties experimentally determined using a series of sulfonated polysulfones. In these materials, the effects of dielectric and Donnan – Manning exclusion on ion sorption were manipulated by

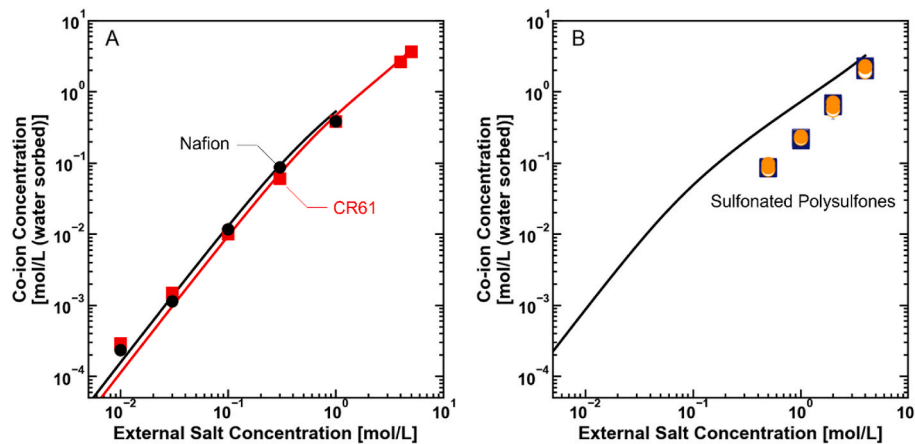


Fig. 1. Co-ion concentration in (A) commercially available CR61 [23] (red squares) and Nafion [27] (black circles) and (B) sulfonated polysulfone (navy squares and orange circles) as a function of external salt solution concentration. The solid lines were calculated for each material using the Donnan – Manning model. The parameters used to model each material are discussed in Section 4.2.1. (For interpretation of the references to colour in this figure legend, the reader is referred to the Web version of this article.)

external salt concentration and synthetic modifications that influenced the dielectric constant and polymer fixed charge concentration. We found that adding dielectric exclusion to the Donnan – Manning model improved agreement with experimental data relative to the Donnan – Manning model alone. In Nafion, adding dielectric exclusion to the Donnan – Manning model improved agreement relative to that of the Donnan – Manning model to a considerably lesser extent than for the sulfonated polysulfones, suggesting that dielectric exclusion may be less relevant in more highly hydrated charged polymers. Overall, the modeling approach described here contributes to efforts to model ion sorption in low water content charged polymers where the Donnan – Manning model is insufficient for describing ion sorption data and dielectric exclusion effects may be important. Insight from the model informs connections between polymer properties and ion exclusion in charged polymers, which may help guide future molecular engineering strategies for polymeric desalination membranes.

2. Theory

Here we outline the modeling approaches used in the subsequent analysis of experimental data. The subsequent sections are applicable to situations where a single salt electrolyte, composed of a monovalent cation and a monovalent anion (e.g., NaCl), is considered. This analysis can, in principle, be generalized or applied to situations involving multivalent ions, though such manipulations are not included here.

Subsequently, we define ion properties as mean ionic values, consistent with how such quantities are described in previous reports [21,34,37,59,62]. This choice was made because experimental techniques used to determine certain colligative properties of ions in polymers only characterize quantities that contain contributions from both cations and anions (e.g., the mean ionic activity coefficients). Mathematically, the analysis in the subsequent section is identical to analysis in other reports where the properties of ions are derived in terms of their individual values [23,27,29,32].

All ion concentrations in the membrane are defined and/or reported in units of mol/L (water sorbed). This definition is denoted by the superscript *w* that accompanies the symbols for all membrane phase concentrations (e.g., the concentration of salt in the membrane, in units of mol/L (water sorbed), is denoted as $C_s^{m,w}$). This distinction is necessary as the definition of the units of concentration can have a significant influence on the analysis of hydrated polymer thermodynamic properties [5,32].

2.1. Donnan equilibrium

The equilibrium condition for a membrane equilibrated with an electrolyte is [21]:

$$\alpha_{\pm}^m = \alpha_{\pm}^s \quad \text{Eq. 1}$$

where α_{\pm}^s is mean ionic activity in the solution and α_{\pm}^m is the mean ionic activity in the membrane. Expressing the mean ionic activity in terms of an activity coefficient and concentration and re-arranging Eq. (1) yields:

$$\frac{\gamma_{\pm}^m}{\gamma_{\pm}^s} = \frac{C_{\pm}^s}{C_{\pm}^{m,w}} \quad \text{Eq. 2}$$

where γ_{\pm}^m and γ_{\pm}^s are the mean ionic activity coefficients in the membrane and solution phases, respectively, and $C_{\pm}^{m,w}$ and C_{\pm}^s are the mean ionic concentrations in the solution and membrane phases, respectively. The mean ionic concentrations are defined using the concentrations of cations (C_+) and anions (C_-). For a salt containing a monovalent cation and a monovalent anion:

$$C_{\pm} = (C_+ C_-)^{1/2} \quad \text{Eq. 3}$$

Similarly, the mean ionic activity coefficients are defined in terms of

the contributions from both cations and anions as $\gamma_{\pm} = (\gamma_+ \gamma_-)^{1/2}$. At equilibrium, the ratio of the concentration of salt in the membrane phase to that of the solution phase is often referred to as the salt sorption (or partition) coefficient, K_s .

The electroneutrality condition states that all positive charges in a phase must be balanced by negative charges in that phase. In monovalent electrolyte solutions, electroneutrality states that the stoichiometric ratio of cations and anions must be equal:

$$C_+^s = C_-^s = C_s^s \quad \text{Eq. 4}$$

where C_s^s defines the concentration of salt in the solution. In a charged membrane with fixed monovalent charges (e.g., sulfonate groups), electroneutrality requires that the stoichiometric ratio of the counter-ions and co-ions is offset by the concentration of the fixed charges, $C_A^{m,w}$ [21]:

$$C_c^{m,w} + C_A^{m,w} = C_g^{m,w} \quad \text{Eq. 5}$$

where $C_c^{m,w}$ is the concentration of co-ions in the polymer, and $C_g^{m,w}$ is the concentration of counter-ions (or gegen-ions) in the membrane. In a cation exchange material, counter-ions are positively charged ions, and co-ions are negatively charged ions. The signs are simply reversed for anion exchange materials.

Therefore, the electroneutrality conditions (Eq. (4), Eq. (5)) can be used to determine the mean ionic concentration in the solution and membrane. In the solution phase, the molar concentration of co- and counter-ions are equal, and as a result, the mean ionic concentration is equal to the solution concentration ($C_{\pm}^s = C_s^s$). In a charged polymer membrane, an expression for the mean ionic concentration in terms of quantities readily measured through experiment (i.e., the co-ion concentration, which is effectively equal to the mobile salt concentration, and fixed charge concentration) is obtained by combining Eq. (5) and Eq. (2):

$$C_{\pm}^{m,w} = [C_c^{m,w} (C_c^{m,w} + C_A^{m,w})]^{\frac{1}{2}} \quad \text{Eq. 6}$$

Substituting the expressions for the mean ionic concentrations in solution and membrane into the condition for electrochemical equilibrium (Eq. (2)) results in the following expression:

$$\frac{\gamma_{\pm}^m}{\gamma_{\pm}^s} = \frac{C_s^s}{[C_c^{m,w} (C_c^{m,w} + C_A^{m,w})]^{\frac{1}{2}}} \quad \text{Eq. 7}$$

which can be used to calculate the mean ionic activity coefficient in the membrane provided that the membrane phase co-ion and fixed charge concentrations are known in addition to the external solution properties (i.e., the concentration and the mean ionic activity coefficient in the external solution). In the analysis of salt transport in membranes, it is often useful to define the mobile ion sorption (or partition) coefficient, K_s , and in ion exchange materials, K_s is taken as the ratio of the concentration of co-ions in the membrane phase to the concentration of salt in the solution phase [2]. Eq. (7) can be rearranged in this way to yield the classic Donnan equation [20,21,37,59]:

$$K_s \equiv \frac{C_s^s}{C_{\pm}^{m,w}} = \left[\frac{1}{4} \left(\frac{C_A^{m,w}}{C_s^s} \right)^2 + \left(\frac{\gamma_{\pm}^m}{\gamma_{\pm}^s} \right)^2 \right]^{\frac{1}{2}} - \frac{1}{2} \frac{C_A^{m,w}}{C_s^s} \quad \text{Eq. 8}$$

Historically, the classic Donnan model has been applied in an idealized form where the ratio of the activity coefficients in Eq. (8) were taken as a constant or unity [20,21,62]. More recently, the importance of these activity coefficients has been more widely realized [26,63], and there has been much consideration of how to properly describe the activity coefficients in the membrane phase. The mean ionic activity coefficient is defined using the molar excess Gibbs free energy of an aqueous salt, \bar{G}_s^E [22,64]:

$$\gamma_{\pm}^j = \exp \left[\frac{\bar{G}_s^{E,j}}{2RT} \right] \quad \text{Eq. 9}$$

where R is the gas constant, T is the absolute temperature, and j is an arbitrary superscript that defines the phase that the salt is in (e.g., solution, s , or membrane, m). The factor of two in Eq. (9) appears because $\bar{G}_s^E = \bar{G}_+^E + \bar{G}_-^E$ [64] and therefore $\bar{G}_s^E = RT \ln(\gamma_{\pm}^2)$, though this factor ultimately cancels out. Inserting Eq. (9) into Eq. (8) yields:

$$\frac{C_c^{m,w}}{C_s^s} = \left[\frac{1}{4} \left(\frac{C_A^{m,w}}{C_s^s} \right)^2 + \left(\exp \left[\frac{-\Delta \bar{G}_{\text{sorption}}^E}{RT} \right] \right) \right]^{\frac{1}{2}} - \frac{1}{2} \frac{C_A^{m,w}}{C_s^s} \quad \text{Eq. 10}$$

where $\Delta \bar{G}_{\text{sorption}}^E$ is the change in the mean ionic partial molar excess Gibbs free energy that is associated with the ion partitioning process (i.e., $\Delta \bar{G}_{\text{sorption}}^E = \bar{G}_s^{E,m} - \bar{G}_s^{E,s}$).

2.2. Donnan – Born Model

When inter-ion and inter-polymer interactions are neglected, the change in excess Gibbs free energy that accompanies the movement of an ion from solution into membrane can be described using the excess solvation energy, ΔW_s (in units of $k_B T$) [22,49,53]:

$$\frac{\Delta \bar{G}_{\text{sorption}}^E}{RT} = \Delta W_s \quad \text{Eq. 11}$$

The excess solvation energy describes the difference between the stored dielectric energy (or self-energy) of an ion in the polymer relative to its value in the bulk (i.e., the solution) [22,51,52]. If the polymer and solution are both considered homogenous dielectric mediums of dielectric constants ϵ_m and ϵ_s , respectively, the Born model can be used to describe the excess solvation energy associated with ion sorption into the material [22,53,54].

Freger recently proposed a reformulation of the classic Born model, where the influence of the local environment experienced by an ion in a polymer (i.e., the presence of additional polymer-solution interfaces within the polymer matrix) is also accounted for in the calculation of the excess solvation energy [53]. In a simplified version of this case, the local environment experienced by an ion in a polymer can be described as a series of solvated cavities (filled with sorbed water) that are distributed throughout the polymer matrix (Fig. 2). Accordingly, the excess solvation energy for the ion is calculated as [53]:

$$\Delta W_i = \frac{z_i^2 e^2}{8\pi \epsilon_0 k_B T r_p} \left(\frac{1}{\epsilon_m} - \frac{1}{\epsilon_s} \right) \quad \text{Eq. 12}$$

where z_i is charge of the ion, e is the elementary charge, ϵ_0 is the vacuum permittivity, and r_p is the characteristic space representing an effective

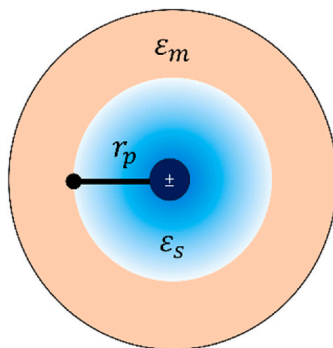


Fig. 2. Born model representation of an ion in a hydrated polymer, placed at the center of a solvated cavity of solution surrounded by the polymer matrix. Adapted from Ref. [53] with permission from Elsevier Ltd.

distance between the low and high dielectric constant regions of the polymer (Fig. 2). An important simplification in the derivation of Eq. (12) is that the solution in the cavity has the same permittivity of that in the bulk, which causes the dependence of the excess solvation energy on the ion size to vanish [53]. In this case, the excess solvation energy of an ion, due to its proximity with the low-dielectric constant polymer, results in a repulsive interaction that repels the ion away from the polymer-solution interface [53]. This interaction is the physical basis for what is commonly referred to as dielectric exclusion.

Because an ion cannot partition into the polymer without an accompanying ion of opposite charge, the total excess solvation energy that describes the ion partitioning process is that for the total salt molecule, ΔW_s (i.e., both the cation and anion). This value is taken as the sum of the individual ion solvation energies [53]:

$$\Delta W_s = \Delta W_+ + \Delta W_- = \frac{z^2 e^2}{4\pi \epsilon_0 k_B T r_p} \left(\frac{1}{\epsilon_m} - \frac{1}{\epsilon_s} \right) \quad \text{Eq. 13}$$

The excess solvation energy calculated via Eq. (13) describes the difference in ionic thermodynamic non-ideality between solution and polymer (via Eq. (11) and Eq. (9)). Given an appropriate value of the mean ionic activity coefficient in the external salt solution, the Born model can be used to predict the mean ionic activity coefficient in the polymer. Similarly, substituting Eq. (13) and Eq. (11) into the Donnan Equation (Eq. 10) results in the Donnan – Born model, which accounts for the influence of Donnan exclusion and dielectric exclusion on ion partitioning [59].

2.3. Donnan – Manning Model

The Manning counter-ion condensation model can also be used to quantify the mean ionic activity coefficients of charged hydrated polymers. Originally, the Manning model was developed to describe interactions between ions in polyelectrolyte solutions. One of the key assumptions used to derive the Manning model is that the polymer chain can be described as a uniformly charged line and that co- and counter-ions only interact with the polymer chain nearest to them [29,31,32]. Despite the simplicity of these geometric assumptions, which seem more reasonable for the highly stretched rod-like polymers in polyelectrolyte solutions than dense charged polymer membranes, the Manning model has yielded reasonable agreement with experimentally determined mean ionic activity coefficients in many, but not necessarily all, desalination-relevant polymers [23,26,27,29,32].

This model relies on the Manning Parameter, ξ , defined as [31]:

$$\xi = \frac{\lambda_B}{b} \quad \text{Eq. 14}$$

where λ_B is the Bjerrum length, and b is the charge spacing parameter, which represents the separation between adjacent fixed charges tethered to the polymer backbone. A critical value of $\xi = 1$ is defined to inform subsequent modeling [29,31]. When the Manning Parameter is less than unity, ion-polymer interactions are described in the Debye-Hückel limit (i.e., described as screened coulombic interactions between ions and charged polymer chains) [29,31]. When the Manning Parameter is greater than unity, a phenomenon referred to as counter-ion condensation occurs, and this interaction, where counter-ions condense along polymer fixed charges to reduce the effective Manning Parameter to unity, is also considered in addition to the interaction described by the Debye-Hückel limit [31].

The mathematical framework of the Manning model treats ion-polymer interactions in a manner similar to the Debye-Hückel limiting law, so the excess free energy due to ion-polymer interactions is calculated as [31]:

$$\frac{F^E}{V k_B T} = -\xi C_A^{m,w} \ln[\kappa] \quad \text{Eq. 15}$$

where F^E is the excess Helmholtz energy, V is the volume of the system, and κ is the characteristic Debye length. The Debye Length describes the length scale over which electrostatic interactions between two charges are screened and is defined as a function of the ionic strength, I , as [65]:

$$\kappa^2 \equiv \frac{4\pi e^2 I}{\varepsilon_0 \varepsilon_m k_b T} = \frac{4\pi e^2}{\varepsilon_0 \varepsilon_m k_b T} (C_A^{m,w} + 2C_c^m) \quad \text{Eq. 16}$$

The effective ionic strength in charged polymers is commonly estimated using the concentration of dissociated co- and counter-ions in the polymer matrix [31,32]. For a charged polymer equilibrated in a 1-1 salt, the ionic strength is effectively equal to the sum of the concentration of co- and counter-ions in the polymer matrix; the right-hand side of Eq. (16) is therefore obtained using the relationship between fixed charge, co-ion, and counter-ion concentration described by the electroneutrality condition (Eq. (6)).

The excess Gibbs free energy and the excess Helmholtz free energy are related as $\Delta G^E = \Delta F^E + \Delta(PV)$ [66,67]. Therefore, the activity coefficients can be obtained from Eq. (15) by taking the pressure-volume work to be negligible and by applying the partial molar operator to the Helmholtz free energy. The error associated with this approximation has been suggested to be negligible and is consistent with the original approach taken by Debye and Hückel [65,66,68].

When the Manning Parameter is less than unity (i.e., counter-ion condensation does not occur and ion-polymer interactions are described in the Debye-Hückel limit) the mean ionic activity coefficient is obtained directly from Eq. (15) as [31]:

$$\gamma_{\pm}^m = \left[\exp\left(-\frac{\xi X}{X+2} \right) \right]^{\frac{1}{2}} \quad \text{Eq. 17}$$

where $X = C_A^m/C_c^m$ [32]. When the Manning Parameter is greater than unity, the mean ionic activity coefficient is calculated as [31]:

$$\gamma_{\pm}^m = \left[\left(\frac{X/\xi + 1}{X+1} \right) \exp\left(-\frac{X}{X+2\xi} \right) \right]^{\frac{1}{2}} \quad \text{Eq. 18}$$

The activity coefficients, calculated using Eq. (18), reflect a physical picture where counter-ions condense onto the fixed charge groups to reduce the Manning parameter to unity, and the interactions between the remaining ions and polymer are described in the Debye-Hückel limit [31]. In many charged polymer membranes, the sharp condensation described by the Manning model is likely non-physical, and rather a distribution of counter-ion states (i.e., condensed or mobile) exist within the charged polymer matrix.

The Donnan – Manning model is obtained by substituting the mean ionic activity coefficient calculated from either Eq. (17) or Eq. (18) into the classic Donnan Equation (Eq. 8) [26]. The Donnan – Manning model is an equation implicit in C_c^m that can be solved analytically for the co-ion concentration that partitions in a polymer. Therefore, at a given value of the fixed charge concentration, external salt concentration, and mean ionic activity coefficient in the external solution (which can be calculated using the Pitzer model [33,34]) the Donnan – Manning model can be used in a predictive fashion [29].

2.4. Donnan – Manning – Born Model

The expression for the excess Helmholtz free energy in the Manning Model (Eq. (15)) is derived from the Poisson-Boltzmann equation (PBE), which is solved via linearization using the Debye-Hückel approximation [31,65]. To develop an activity coefficient model that accounts for interactions described by the Manning model and dielectric exclusion, we derived an expression for the excess Helmholtz free energy using a form of the PBE modified to include the excess solvation energy of an ion (Eq. S1) [58]. This PBE was also solved using the Debye-Hückel approximation (Section S1), and to do that, the excess solvation energy was taken as a constant that is described by the Born Model (Eq. (13)). The

approximation of constant excess solvation energy is an oversimplification of the physics describing ionic interactions in the polymer (for example, theory developed by Yaroshchuk suggests that interactions between ions and polarization charges may be screened by the Donnan potential [58]). This approximation, however, is valuable as it provides an analytical way to describe the influence of dielectric exclusion, counter-ion condensation, and Donnan exclusion on experimentally determined ion sorption properties of charged polymers.

The excess Helmholtz free energy, modified to include the constant excess solvation energy of an ion, is:

$$\frac{F^E}{V k_b T} = -\xi C_A^{m,w} \left(\ln[\kappa] - \frac{\Delta W_i}{2} \right) \quad \text{Eq. 19}$$

Here, the Manning parameter serves the same function as in the original Manning model, and a critical value of $\xi = 1$ is defined to determine whether counter-ions condense along the polymer fixed charges. When the Manning parameter is less than unity, the mean ionic activity coefficients are determined using Eq. (19) as:

$$\gamma_{\pm}^m = \left[\exp\left(-\frac{\xi X}{X+2} + \xi C_A^{m,w} \Delta W_s \right) \right]^{\frac{1}{2}} \quad \text{Eq. 20}$$

and when the Manning parameter is greater than unity, the mean ionic activity coefficients are calculated as:

$$\gamma_{\pm}^m = \left[\left(\frac{X/\xi + 1}{X+1} \right) \exp\left(-\frac{X}{X+2\xi} + \frac{C_A^{m,w}}{\xi} \Delta W_s \right) \right]^{\frac{1}{2}} \quad \text{Eq. 21}$$

Both Eq. (20) and Eq. (21) are determined from Eq. (19) in the same manner that Eq. (17) and Eq. (18) are determined from Eq. (15). The derivations of each equation are discussed further in Section S1. The Donnan – Manning – Born model is also obtained by substituting the mean ionic activity coefficient calculated from Eq. (20) or Eq. (21) into the Donnan Equation (Eq. 8), and the result is also an equation implicit in C_c^m , which is solved in the same manner as in the Donnan – Manning model.

3. Materials and methods

3.1. Materials

Two series of sulfonated poly(aryl ether sulfone) random copolymers were synthesized using a nucleophilic step growth reaction reported previously [37]. The co-monomers were either sulfonated (3, 3'-disulfonated-4,4'-dichlorodiphenylsulfone (SDCDPS, >99 %, Akron Polymer Systems)) or non-sulfonated (4,4'-dichlorodiphenylsulfone (DCDPS, 98 %, Sigma-Aldrich)). The sulfone co-monomers were joined using either hydroquinone (HQ, >99 %, Sigma-Aldrich), methoxy-hydroquinone (MHQ, >99 %, Sigma-Aldrich), or biphenol (4,4'-biphenol (BP), 97 %, Acros Organics) linkages. The first series of polymers, which did not contain methoxy group functionality, were synthesized using a 2:3 M ratio of HQ:BP. The second series of polymers, which contained methoxy groups, were synthesized using a 2:3 M ratio of MHQ:BP. The order that sulfonated or non-sulfonated co-monomers and linkages were joined was likely random [11,45,69], and the general structures are reported below (Table 1). Polymer structural verification via ^1H NMR was reported previously [37].

The degree of sulfonation, controlled by varying the ratio of sulfonated to non-sulfonated co-monomers, was 20 %, 25 %, or 30 % (Table 1). The degree of disulfonation is represented by XX in the polymer nomenclature: HQ:BP – XX and MHQ:BP – XX. The degree of disulfonation directly informs the ion exchange capacity (IEC) of the polymer, and materials were prepared with IECs ranging from 0.81 to 1.19 mEq/g (dry polymer) (Table 1).

Polymer film samples were solution cast from a 5 % (w/v) solution of polymer in anhydrous *N,N*-dimethylacetamide (DMAc, 99.8 %, Fisher

Table 1

Properties and chemical structures of HQ:BP – XX and MHQ:BP – XX. Reported ion exchange capacity (IEC) values were calculated according to the synthetic recipe (i.e., by assuming the ratio of non-sulfonated to sulfonated co-monomers in the final polymer were equal to the ratio of DCDPS to SDCDPS initially added to the reaction mixture). The uncertainty in the water volume fractions was taken as the standard deviation from the mean of three measurements.

Material	IEC ^a	Water volume fraction, φ_w ^b	Chemical structure
HQ:BP – 20	0.83	0.15 ± 0.01	
HQ:BP – 25	1.01	0.20 ± 0.01	
HQ:BP – 30	1.19	0.24 ± 0.01	
MHQ:BP – 20	0.81	0.14 ± 0.01	
MHQ:BP – 25	0.99	0.19 ± 0.01	
MHQ:BP – 30	1.16	0.25 ± 0.01	

^a Calculated by assuming that the polymer is in the Na^+ counter-ion form and reported in units of meq/g (dry polymer).

^b For polymers equilibrated with DI water.

Chemical). The casting solutions were prepared by mixing polymer and solvent until the polymer dissolved completely, and then, the solutions were filtered through a 1 μm poly(tetrafluoroethylene) (PTFE) syringe filter. Films were cast by pouring the filtered casting solution into 6 cm diameter circular PTFE molds.

To form solid polymer films, solvent was removed via a two-step drying process. First, the solution in the molds was heated in a convection oven at 80 °C for at least 24 h to remove most of the solvent and form a solvated polymer film. Next, the samples were placed under vacuum and dried for an additional 24 h at 80 °C. After these drying steps, the samples were equilibrated in de-ionized (DI) water (18.2 MΩ cm) for at least 24 h. This equilibration step allowed the samples to fully hydrate, and it facilitated extraction of residual solvent from the polymer.

3.2. Water content and fixed charge concentration

First, the wet masses, m_{wet} , of hydrated samples equilibrated with either 0.5 M, 1 M, 2 M, or 4 M NaCl were measured. The hydrated polymer samples were dried under vacuum at 80 °C for 24 h to remove water from the polymer. These drying conditions were verified to sufficiently remove water from the polymer matrix by ensuring that allowing the drying process to proceed longer did not appreciably influence the mass of the dry polymer [37]. After drying, the samples were weighed quickly to determine the mass of dry polymer, m_{dry} , and the water uptake was calculated as [37,38,46]:

$$w_u = \frac{m_{\text{wet}} - m_{\text{dry}}}{m_{\text{wet}}} \quad \text{Eq. 22}$$

Immediately thereafter, the polymers were submerged and weighed in cyclohexane, an auxiliary solvent that does not readily partition into sulfonated polysulfone over the timescale of the experiment [45]. This mass, m_{aux} , was used to determine the dry density of the polymers, ρ_p via Archimedes' Principle as [37,38,46]:

$$\rho_p = \frac{m_{\text{dry}}}{m_{\text{dry}} - m_{\text{aux}}} (\rho_{\text{aux}} - \rho_{\text{air}}) + \rho_{\text{air}} \quad \text{Eq. 23}$$

where ρ_{aux} and ρ_{air} are the densities of cyclohexane air, respectively. The measurement temperature was recorded for each measurement, and it was 22 ± 1 °C. The values of ρ_{aux} and ρ_{air} used in Eq. (23) were taken as 0.789 g/cm³ and 0.0012 g/cm³, respectively, at 22 °C [70].

Using the water uptake data and IEC, the concentration of fixed charge groups in the polymer can be calculated as [71]:

$$C_A^{m,w} = \frac{\text{IEC} \times \rho_w}{w_u} \quad \text{Eq. 24}$$

where $C_A^{m,w}$ is the fixed charge concentration in [mol (L water sorbed)⁻¹]. Using the polymer dry density and water uptake data, the polymer water volume fraction, φ_w , is calculated as [46]:

$$\varphi_w = \frac{w_u}{w_u + \frac{\rho_w}{\rho_p}} \quad \text{Eq. 25}$$

where ρ_w was the density of water (1.0 g/cm³). A volume additivity assumption is taken to calculate the water volume fraction in Eq. (25), (i.e., the total volume of hydrated polymer was taken to be equal to the sum of the volumes of polymer and sorbed water) [72].

3.3. Microwave dielectric relaxation spectroscopy

The frequency dependent relative permittivity properties of the hydrated polymers were characterized using microwave dielectric relaxation spectroscopy (DRS) [55,57,73,74]. The measurements were made using a vector network analyzer (VNA), which generated and subjected hydrated polymer samples to an oscillating electromagnetic field in the microwave frequency range (45 MHz–26.5 GHz). Coaxial transmission lines were used to carry the electromagnetic signals from the VNA to the polymer, where they were either reflected by or transmitted through the polymer, and to carry the reflected/transmitted signals back to the VNA [55]. From these signals, the VNA generated a series of S-parameters, which are mathematically related to the relative complex permittivity. The dielectric constant was determined using the low-frequency limit of the real component of the complex permittivity [55].

To prepare the samples for DRS, hydrated polymer films equilibrated with either 0.5 M, 1 M, 2 M, or 4 M NaCl were cut into rectangular strips with a 0.5 cm width. The coaxial transmission line sample holder (a 3.5 mm diameter outer conductor with a 1.52 mm diameter inner conductor at its center) was filled with these polymer samples by wrapping the strips around the inner conductor [55,57]. To ensure that there were no air gaps in the sample holder, which could introduce measurement artifacts [57,74], the polymers were wrapped until all of the annular space between the inner and outer conductors was filled.

3.4. Mobile salt concentration

The concentrations of ions that partition into the polymers at equilibrium with either 0.5 M, 1 M, 2 M, or 4 M NaCl were measured using a desorption technique [20,45,75,76]. First, to calculate the volume of the swollen polymer samples, the diameter and thickness of circular sample disks, equilibrated with salt solution, were measured using digital calipers (Item No. 293–344, Mitutoyo). Then, excess NaCl solution was wiped from the surface of the films, and the samples were placed into a desorption solution containing 100 mL of initially DI water that was equilibrated under atmospheric conditions for at least 48 h. The desorption solution was stirred at 400 RPM to facilitate extraction of salt from the polymer into this desorption solution. The conductivity of the desorption solution, which is proportional to the concentration of NaCl in the solution, was measured until it remained constant for at least a period of time equal to the characteristic timescale for diffusion in the sample. This criterion was chosen as a standard marker for the point where salt desorption from the polymer had effectively stopped. The

desorption solution temperature was held constant at 22 ± 0.1 °C by means of a jacketed beaker and a temperature-controlled circulator because the relationship between solution conductivity and salt concentration depends on temperature.

In charged polymers, most of the counter-ions sorbed in the polymer cannot desorb because they must remain in the polymer to preserve electroneutrality with the fixed charge groups. The counter-ions that do desorb from the polymer are those counter-ions that maintain electroneutrality with the desorbed co-ions (i.e., the so-called mobile salt) [20]. Thus, the final salt concentration of the desorption solution can be used to determine the mobile salt concentration in the external salt solution equilibrated polymer, as:

$$C_c^m = C_s^m = \frac{C_d V_d}{V_p \varphi_w} \quad \text{Eq. 26}$$

where C_d is the final salt concentration of the desorption solution, V_d is the desorption solution volume (i.e., 100 mL), and V_p is the swollen polymer volume. The co-ion concentration calculated via Eq. (26) is in units of $[(\text{mol}/\text{L water sorbed})^{-1}]$.

4. Results and discussion

4.1. Experimental

4.1.1. Water content and fixed charge concentration

The water content of the HQ:BP – XX and MHQ:BP – XX polymers depended both on the degree of disulfonation and on the composition of the external solution in equilibrium with the material. Polymer water uptake increased with degree disulfonation (Fig. 3) consistent with previous sulfonated polysulfone observations [45]. The fixed charge concentration, however, decreased with increasing degree disulfonation (Fig. 4) because increases in the dry polymer basis concentration of sulfonate groups led to increases in swelling that diluted the volumetric concentration of fixed charges in the material (Eq. (24)). The inclusion of methoxy groups on the polymer backbone caused the water uptake in the MHQ:BP – XX polymers to be lower than those in HQ:BP – XX (for example, MHQ:BP – 30 and HQ:BP – 30 polymers equilibrated with 0.5 M NaCl had water uptakes of 0.23 and 0.26 [g (water)/g (dry polymer)], respectively) (Fig. 3). As a result, the MHQ:BP – XX polymers had larger fixed charge concentrations than the HQ:BP – XX polymers (MHQ:BP – 30 and HQ:BP – 30 polymers equilibrated with 0.5 M NaCl had fixed charge concentrations of 5 and 4.5 [eq. (fixed charge)/L (water sorbed)], respectively) (Fig. 4) [37].

Polymer water uptake decreased with increasing external salt concentration (Fig. 3) due to osmotic de-swelling. Osmotic de-swelling describes a phenomenon where the water uptake in the polymer decreases due to the reduction of water activity in the external solution, which occurs as salt concentration increases [23,77,78]. Osmotic de-swelling causes the fixed charge concentration to increase with increasing salt concentration (Fig. 4) because the fixed charges in the polymer are concentrated by the decreased water uptake (Eq. (24)).

Out of the three independent variables, the external salt concentration and fixed charge concentration influenced the polymer water uptake and fixed charge concentrations most significantly, but the influence of methoxy group incorporation on these properties was less significant. Increasing the external salt concentration from 0.5 M to 4 M NaCl caused the water uptake of HQ:BP – 25 to decrease by approximately 25 % and the fixed charge concentration to increase by approximately 40 %. Likewise, increasing the degree disulfonation (from XX = 20 to XX = 30), caused the water uptake of the HQ:BP polymers to increase by approximately 50 % and the fixed charge concentration to decrease by approximately 30 %. However, at a given salt concentration and degree disulfonation, the magnitude of the percent change of the water uptake and fixed charge concentrations as a result of methoxy group incorporation of the polymers were considerably smaller. For example, the water uptake and fixed charge concentration of MHQ:BP – 30 relative to that of HQ:BP – 30 both changed by approximately 10 % (and generally, this change was similar in magnitude to the uncertainty associated with the measurements).

4.1.2. Dielectric constant

The dielectric constant increased as the degree of disulfonation increased (Table 2). This result is qualitatively consistent with previous observations where the dielectric constant of hydrated polymers increases as polymer water content increases as a result of greater degrees of disulfonation (Fig. 3) [46,55]. The dielectric constants of the MHQ:BP – XX polymers were lower than those values for the corresponding HQ:BP – XX polymers (Table 2). This result suggests that incorporating polar methoxy groups along the polysulfone backbone is a molecular engineering strategy that reduces the polymer dielectric constant [37].

For a given polymer, the dielectric constant was statistically independent of the external salt concentration (Table 2). This finding is consistent with previous measurements of the relative permittivity properties of hydrated polymers where the dielectric constant was found to be independent of the concentration of salt in the external electrolyte solution [56]. The dielectric constant of aqueous electrolyte solutions

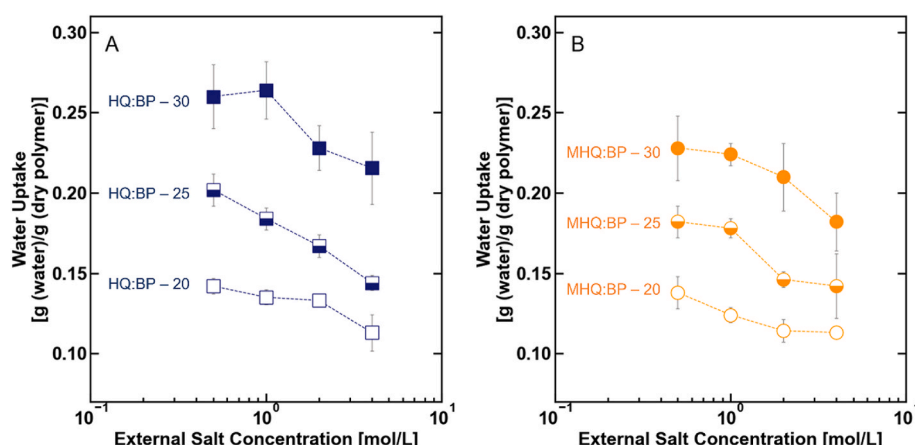


Fig. 3. Water uptake for (A) HQ:BP – 20 (□), HQ:BP – 25 (■), and HQ:BP – 30 (■) and (B) MHQ:BP – 20 (○), MHQ:BP – 25 (●), MHQ:BP – 30 (●) reported as a function of external salt concentration. The lines are intended to guide the eye. The uncertainties were taken as the standard deviation from the mean of three measurements.

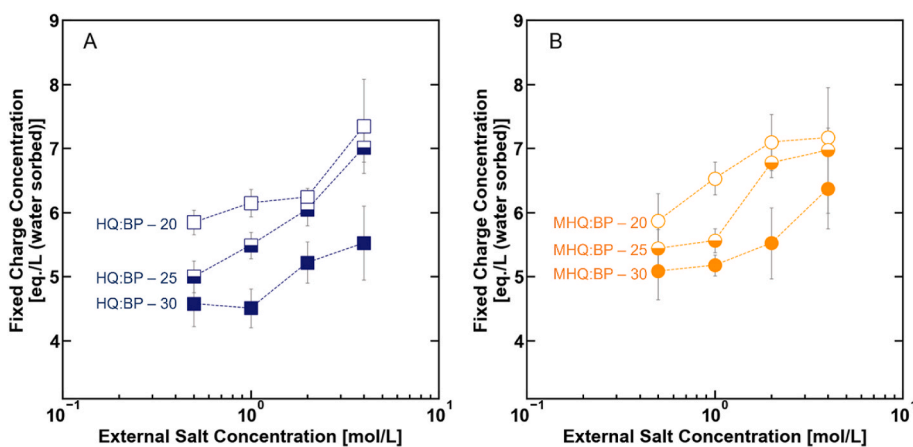


Fig. 4. Fixed charge concentration for (A) HQ:BP – 20 (□), HQ:BP – 25 (□), and HQ:BP – 30 (■) and (B) MHQ:BP – 20 (○), MHQ:BP – 25 (●) MHQ:BP – 30 (●) reported as a function of external salt concentration. The lines are intended to guide the eye. The uncertainties in the values, which were determined using Eq. (24), were calculated via error propagation.

Table 2

Dielectric constants of the HQ:BP – XX and MHQ:BP – XX polymers equilibrated with 0.5 M–4 M NaCl solutions. The uncertainties were taken as the standard deviation from the mean of three measurements.

Material	Dielectric constant			
	0.5 M NaCl	1 M NaCl	2 M NaCl	4 M NaCl
HQ:BP – 20	4.3 ± 0.2	4.0 ± 0.5	3.6 ± 0.4	3.6 ± 0.2
HQ:BP – 25	5.4 ± 0.5	5.5 ± 0.7	5.5 ± 0.4	4.8 ± 0.6
HQ:BP – 30	7.5 ± 0.2	7.0 ± 0.4	7.2 ± 0.4	6.8 ± 0.2
MHQ:BP – 20	3.1 ± 0.1	3.2 ± 0.2	3.2 ± 0.3	3.5 ± 0.3
MHQ:BP – 25	4.0 ± 0.15	3.8 ± 0.2	4.3 ± 0.3	4.1 ± 0.3
MHQ:BP – 30	5.0 ± 0.5	5.8 ± 0.1	5.2 ± 0.2	5.3 ± 0.5

generally decreases as external salt concentration increases [79], so overall, these results provide additional evidence that salt concentration may influence the dielectric constant of hydrated polymers in a different manner than in aqueous electrolyte solutions.

4.1.3. Mobile salt concentration

The co-ion (i.e., mobile salt) concentration (in units of mol/L (water

sorbed)) increased with degree disulfonation by approximately 5–15 % from HQ:BP – 20 to HQ:BP – 30 (Fig. 5A) and approximately 10–25 % from MHQ:BP – 20 to MHQ:BP – 30 (Fig. 5B) over the range of external salt concentrations investigated. Because the fixed charge concentration decreases with degree disulfonation (Fig. 4), this result suggests that increasing the polymer fixed charge concentration suppresses mobile ion sorption in the sulfonated polysulfones, which is qualitatively consistent with the relationship between fixed charge concentration and ion sorption properties determined in other polymers [71]. The co-ion concentrations were statistically equivalent between the HQ:BP – XX and MHQ:BP – XX polymers (Fig. 5), suggesting that methoxy group incorporation (and the suppression of the polymer dielectric constant achieved through the methoxy group incorporation) did not appreciably influence ion sorption in these measurements.

Co-ion concentrations increased with external salt concentration (Fig. 5). This observation is also consistent with previous observations of salt partitioning properties of sulfonated polymers [20,26]. Like the observations for the water uptake and fixed charge concentration, external salt concentration did not affect the relationships between polymer structural elements (i.e., degree disulfonation and methoxy group incorporation) on the co-ion concentration (Fig. 5).

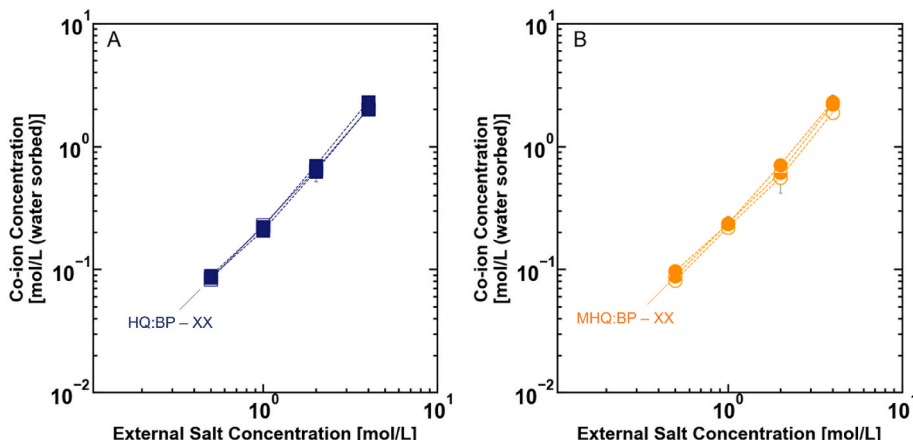


Fig. 5. Mobile salt concentrations for (A) HQ:BP – 20 (□), HQ:BP – 25 (□), and HQ:BP 30 (■) and (B) MHQ:BP – 20 (○), MHQ:BP – 25 (●) MHQ:BP – 30 (●) reported as a function of external salt concentration. The uncertainties were taken as the standard deviation from the mean of three measurements.

The finding that the co-ion concentration in the sulfonated polysulfones was proportional to the ratio of external solution concentration and fixed charged concentration (i.e., $C_c^m \sim C_s^s/C_A^m$) is qualitatively consistent with Donnan exclusion theory and suggests that, to a first approximation, the Donnan equation (Eq. 8) describes the ion sorption properties of the sulfonated polysulfones [21,80]. Alternatively, the result that the co-ion concentration in the sulfonated polysulfone was not influenced by polymer dielectric constant suppression via methoxy group incorporation is not qualitatively consistent with the dielectric exclusion described by the Donnan – Born model, which suggests that co-ion sorption should decrease as the polymer dielectric constant is reduced (Section 2.2). Given that the Donnan – Manning model does not fully describe the ion sorption properties of the sulfonated polysulfones either (Fig. 1), it is unclear which thermodynamic interactions influence mobile salt partitioning in the sulfonated polysulfones. The following sections aim to answer this question by quantitatively analyzing the applications of the Donnan – Born, Donnan – Manning, and Donnan – Manning – Born models to HQ:BP – XX and MHQ:BP – XX.

4.2. Modeling

The mean ionic activity coefficients in a hydrated polymer can be described using the Born model (Eq. (12)), Manning model (Eq. (18)) or Manning – Born model (Eq. (21)). The Born model describes the influence of interactions between ions and their induced polarization charges on the mean ionic activity coefficients, and these interactions are unfavorable for ions when the dielectric constant of hydrated polymer is less than that in the external solution (i.e., $\epsilon_m < 80$) (Fig. 6). Alternatively, the Manning model accounts for interactions between ions and polymer chains, which are inherently favorable (Fig. 6).

At low values of the dielectric constant, the Born model predicts that

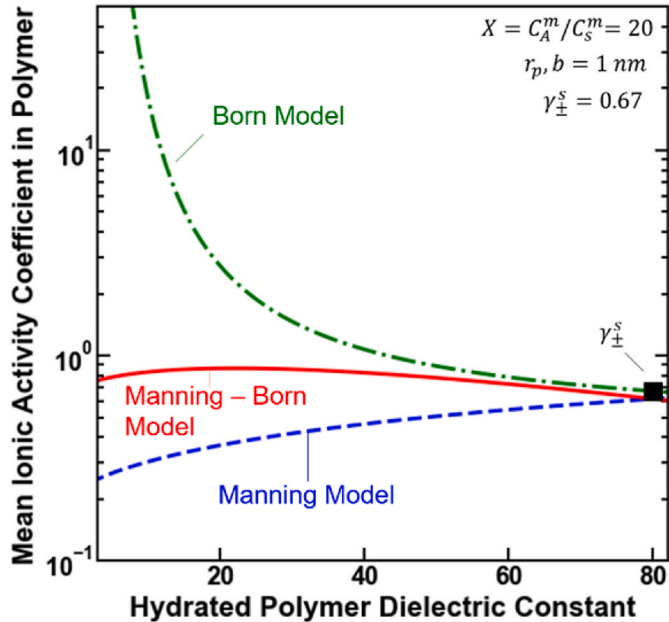


Fig. 6. Born, Manning, and Manning – Born model calculations describing how the mean ionic activity coefficient depends on the dielectric constant. In these calculations, the mean ionic activity coefficient of the external solution was set at its value for a 1 M NaCl solution (i.e., 0.67 determined via the Pitzer model), and the dimensionless parameter X was held constant at 20, which generally is consistent with values for a typical ion exchange membrane equilibrated with 1 M NaCl external salt solution concentration. The application of this model therefore represents a hypothetical case where the external salt solution concentration (and thus, concentration of salt in the membrane) is constant, and the thermodynamic properties of the hydrated polymer matrix are only influenced by variations in the polymer dielectric constant.

the magnitude of the excess solvation energy is larger than that at high values of the dielectric constant. As a result, the mean ionic activity coefficients increase in magnitude (in the non-ideal, un-favorable direction) as the dielectric constant decreases (Fig. 6). In the Manning model, however, the Bjerrum length becomes larger as the dielectric constant decreases (Eq. (16)), and this situation leads to more counterion condensation as the dielectric constant decreases [31]. As a result, the Manning model predicts that the mean ionic activity coefficients become more non-ideal in the favorable direction as the dielectric constant decreases (Fig. 6). Both the Born and Manning models predict that the mean ion activity coefficients approach ideality as the dielectric constant increases and approaches that of the external solution (Fig. 6).

The Manning – Born model describes ionic non-ideality resulting from both the interactions between ions and their induced polarization charges and ions and the polymer (Section 2.4). Accounting for both interactions (which influence the ionic non-ideality in competing directions) causes the ion activity coefficients predicted by the Manning – Born model to remain more ideal than those predicted using either the Manning model or Born model in the range of dielectric constants relevant for sulfonated polysulfones (i.e., $\epsilon_m < 10$ (Table 2)) (Fig. 6). When the dielectric constant is equal to the dielectric constant of the solvent (denoted by the sole square point in Fig. 6), the mean ionic activity coefficient predicted via the Born model approaches the mean ionic activity coefficient in the external solution (i.e., the excess solvation energy equals zero and ion-solvent interactions are ideal). In this situation, the excess solvation energy does not contribute to the ion sorption process, and the ionic activity coefficient predicted via the Manning – Born model converges with that predicted by the Manning model (Fig. 6).

4.2.1. Model application and simplifications

To apply the Born, Manning, and Manning – Born models to the experimental mean ionic activity coefficient data for the sulfonated polysulfones, two simplifications were made to reduce the complexity of modeling the series of materials over the 0.5–4 M NaCl range. First, each model was applied to the sulfonated polysulfones using a single set of parameters that describes all six structural conformations of the sulfonated polysulfones. These parameters – specifically, the fixed charge concentration, dielectric constant, and charge spacing – were taken as their average value over the entire series (Table 3). This simplification had a minor impact on the accuracy of the models (Section S2), which is not surprising based on the previous observations that the external salt concentration generally influenced material properties (e.g., ion sorption and fixed charge concentration) more significantly than the degree disulfonation and methoxy group incorporation. The second simplification was that the fixed charge concentration, dielectric constant, and charge spacing parameters used for all materials were taken as their values in their most hydrated state (i.e., when equilibrated with DI water) (Table 3). While this simplification is consistent with applications of the Donnan – Manning model in the literature [23,26,27], certain parameters, such as the polymer fixed charge concentration, are influenced by the external salt concentration. The influence of this simplification on the model is discussed further in the supporting information (Section S3).

The models were also applied to Nafion 212, a commercially available sulfonated perfluorinated polymer. Nafion is a good comparison material to understand the relevance of dielectric exclusion in a wide range of polymers because previous investigations from Sujianani et al. suggest that the Donnan – Manning model describes the ion sorption properties of Nafion with a high degree of accuracy (Fig. 1) [27]. The parameters for the models applied to Nafion were taken as reported (Table 3) [27]. The parameters used to apply the Manning model to CR61 (Fig. 1) are provided for reference (and were taken as their values reported by Galizia et al. [23]); however, the dielectric constant for those polymers was not directly measured, so the Born and Born – Manning models were not applied to CR61.

Table 3

Parameters used in the application of Donnan – Born, Donnan – Manning, and Donnan – Manning – Born models to the experimental data for the sulfonated polysulfone polymers and Nafion 212. The parameters used to model the sulfonated polysulfone data were estimated using their average value for the entire series of HQ:BP – XX and MHQ:BP – XX polymers. The parameters used to model Nafion 212 were taken as their values reported by Sujanani et al. [27].

Material	Fixed Charge Concentration ^a , $C_A^{m,w}$	Dielectric Constant, ϵ_m	Charge Spacing Parameter ^b , b	Manning Parameter, ξ	Characteristic Space ^{b,c} , r_p
Sulfonated polysulfone	5.3	4.65	0.66	19	0.75
Nafion 212	3.96	20	0.9	3.2	2.5
CR61	3	42 ^d	0.73	1.83	–

^a Units of [eq./L (water sorbed)].

^b Units of [nm].

^c Estimated as the half of the characteristic spacing measured via small angle neutron scattering (SANS).

^d Estimated based on polymer water volume fraction [23].

The agreement between model predictions and experimental data was analyzed in terms of the root-mean-square (RMS) log error, which was calculated as [29]:

$$\text{RMSlogerror} = \sqrt{\frac{1}{n} \sum_{i=1}^n \left(\log \left(\frac{C_{c, \text{experimental}}^i}{C_{c, \text{predicted}}^i} \right) \right)^2} \quad \text{Eq. 27}$$

where n is the number of datum in the dataset, and the limits of the summation C_s^i - C_s^n represent the external salt concentration range that the dataset is collected/predicted over. For example, for the averaged sulfonated polysulfone data set, C_s^i - C_s^n is 0.5 M–4 M NaCl, and n is 24 (because there are 6 structural conformations of the sulfonated polysulfones in the entire series). As discussed by Kitto and Kamcev, the RMS log error is chosen to represent the visual agreement between the experimental data and model predictions on a log-log ion partitioning plot [29]. For reference, a data point with a RMS log error of 0.0 is identical to its predicted value and a data point with a RMS log error of 1.0 is either over-predicted by 900 % or under-predicted by 90 % of its true value [29].

4.2.2. Donnan – Born Model

The two important parameters that influence ion sorption in the Donnan – Born model are the dielectric constant (Section 4.1.2) and the characteristic spacing parameter (Fig. 2). The characteristic spacing parameter was estimated as 0.75 for the sulfonated polysulfones and 2.5 for Nafion; these values are half of the correlation length determined using Small Angle Neutron Scattering (SANS) performed on a series of similarly structured sulfonated polysulfones and Nafion [81,82]. The correlation length is a material property that describes the separation

between hydrophilic and hydrophobic regions of hydrated polymers [83–85] and is believed to be a reasonable estimate for the value of r_p (Fig. 2).

The Donnan – Born model under-predicts the mobile salt concentration in the sulfonated polysulfones by at least five orders of magnitude (Fig. 7A) resulting in an RMS log error of 14.7 (Table 4). This result is reasonable given that the Born model over-predicts the mean ionic activity coefficients (i.e., suggests they are more non-ideal in the non-favorable direction) by at least three orders of magnitude (Fig. 8A). These large deviations between the Born model and experimental data occur because, in low dielectric constant sulfonated polysulfones, the Born model predicts that the excess solvation energy – or degree of ionic non-ideality in the non-favorable direction – is large and positive (Fig. 6), and it neglects the influence of favorable interactions between counter-ions and fixed charges that cause favorable ionic non-ideality.

While the Donnan – Born model also under-predicted the co-ion

Table 4

Root-mean-square (RMS) Log error between the Donnan – Born, Donnan – Manning, and Donnan – Manning – Born predictions and the experimentally determined co-ion concentration. RMS log errors were calculated as described by Kitto and Kamcev [29].

Material	Model	RMS log error
Sulfonated Polysulfone	Donnan – Born	14.7
	Donnan – Manning	0.93
	Donnan – Manning – Born	0.34
Nafion 212	Donnan – Born	2.11
	Donnan – Manning	0.30
	Donnan – Manning – Born	0.26

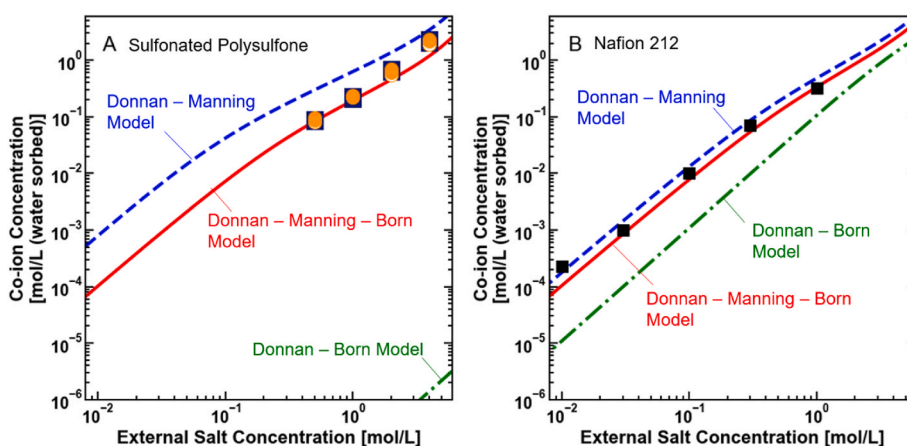


Fig. 7. Mobile salt concentration for the sulfonated polysulfones (A) (HQ:BP – 20 (□), HQ:BP – 25 (■), HQ:BP 30 (■), MHQ:BP – 20 (○), MHQ:BP – 25 (○) and MHQ:BP – 30 (●)) and (B) Nafion 212 (■) plotted as a function of external salt concentration. Lines represent calculations made using the Donnan – Born, Donnan – Manning and Donnan – Manning – Born models.

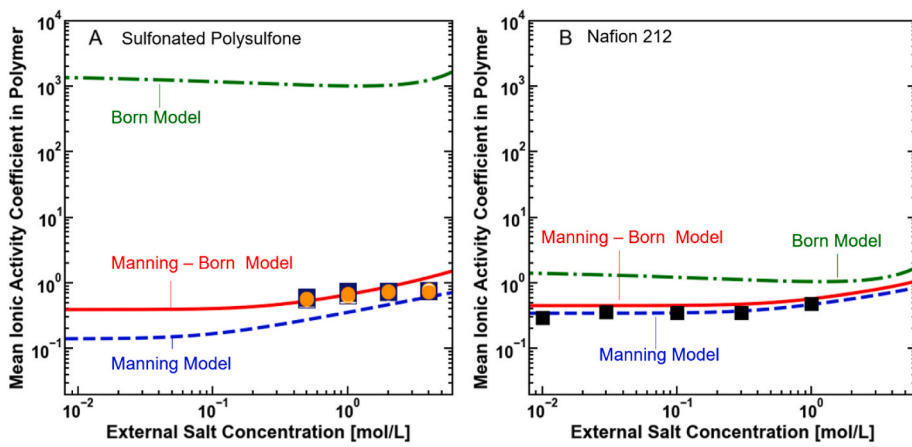


Fig. 8. Mean ionic activity coefficients measured for the (A) sulfonated polysulfones (HQ:BP – 20 (□), HQ:BP – 25 (□), HQ:BP 30 (■), MHQ:BP – 20 (○), MHQ:BP – 25 (●) and MHQ:BP – 30 (●)) and (B) Nafion 212 (■) plotted as a function of external salt concentration. Lines are plotted as the Donnan – Born, Donnan – Manning and Donnan – Manning – Born predictions for the mean ionic activity coefficients of each material.

concentration in Nafion (Fig. 7B) (i.e., the Born model over-predicts the mean ionic activity coefficients (Fig. 8B)), the predictions were more accurate than that for the sulfonated polysulfones (i.e., had a RMS log error of 2.11, which is considerably lower than that of the sulfonated polysulfone (Table 4)). Nafion has a larger dielectric constant and characteristic space relative to the sulfonated polysulfones (Table 3), which reduces the Born model predictions for the excess solvation energy and mean ionic activity coefficients of a given ion (Eq. (13)). As a result, the Born model suggests that the mean ionic activity coefficients deviate from ideality in the non-favorable direction to a lesser extent than in the sulfonated polysulfones, and the Donnan – Born predictions of the co-ion concentrations are more realistic in Nafion than sulfonated polysulfone.

4.2.3. Donnan – Manning Model

The two important parameters that influence ion sorption in the Donnan – Manning model are the dielectric constant and the charge spacing parameter (Section 2.1.3). The charge spacing parameter for the sulfonated polysulfones was estimated using results reported by Vondrasek et al. where the charge spacing parameter in a similarly structured series of sulfonated polysulfones was related to the sulfonate group hydration (Section S4) [86]. For all combinations of the dielectric constant and charge spacing parameters in the sulfonated polysulfones and Nafion, the Manning parameter was greater than unity (Table 3), so Eq. (18) was used to calculate the mean ionic activity coefficients.

Contrary to the Donnan – Born model, the Donnan – Manning model over-predicts the mobile salt concentration in the sulfonated polysulfone (RMS log error of 0.93) (Fig. 7A–Table 4) because the Manning model under-predicts the mean ionic activity coefficients (Fig. 8A). In the low dielectric constant sulfonated polysulfones, the Manning model suggests that the mean ionic activity coefficients deviate from ideality in the favorable direction to a large extent (Fig. 6). However, the magnitude of the deviation from non-ideality in the non-favorable direction due to dielectric exclusion is also large in this low-dielectric constant regime (Fig. 6), and as a result, neglecting dielectric exclusion results in the under-prediction of the mean ionic activity coefficients and resulting over-prediction of ion sorption.

The visual agreement between the Donnan – Manning predictions and experimental data increases with increasing external salt concentration (Fig. 6). In other IEMs, the accuracy of the Manning model also improved with increasing salt concentration [23,26,29]. The increase in accuracy is likely related to a simplifying assumption made in the derivation of the Manning model, where only interactions between ions

and their nearest-neighbor polymer chain are considered [31]; this assumption becomes more reasonable as the ionic strength of solution increases and interactions between ions and distant polymer chains are sufficiently screened [23,26].

The Donnan – Manning model describes the thermodynamic properties of NaCl in Nafion (RMS log error of 0.30 (Table 4)) more accurately than those of the sulfonated polysulfone. In the range of dielectric constants relevant for Nafion, the Born-model contributions to the mean ionic activity coefficients approach unity (Fig. 6), suggesting that dielectric exclusion does not contribute significantly to ionic non-ideality in these materials. These results are consistent with previous explanations of ion sorption in highly charged, high dielectric constant polymers, where primary ionic interactions (here, ion-polymer interactions described by the Manning model) govern ionic non-ideality, and secondary interactions (such as those between ions and polarization charges) are less relevant.

4.2.4. Donnan – Manning – Born Model

The Donnan – Manning – Born model predicts the co-ion concentration in the sulfonated polysulfones with a higher degree of accuracy (i.e., the lowest RMS log error) compared to either the Donnan – Born or Donnan – Manning models alone (Fig. 7A–Table 4). This result is due to the fact that the Manning – Born model more accurately describes the mean ionic activity coefficients in the sulfonated polysulfone (Fig. 8A). As such, ion interactions with induced polarization charges and ion-polymer interactions are likely important influencers for ion sorption in sulfonated polysulfone.

The agreement between the Donnan – Manning – Born predictions and experimental data decreases as the external salt concentration increases. For polymers equilibrated with the 2 M and 4 M NaCl solutions, the Donnan – Manning – Born model under-predicts ion sorption and the Manning – Born model over-predicts the mean ionic activity coefficients. This inaccuracy may occur due to the assumption in the derivation of the model that the excess solvation energy is a constant that is not influenced by the ionic strength of the solution. This assumption may break down in higher concentration salt solutions. For example, although the dielectric constant of the polymers did not change with external salt solution (Section 4.1.2), the dielectric constant of aqueous NaCl decreases from 80 in the limit of infinite dilution to approximately 50 in 4 M NaCl [79,87], and the decrease of the relative permittivity of solution suggests that the excess solvation energy decreases with increasing salt concentration (Eq. (12)). Accounting for the concentration dependence of the relative permittivity in models that describe electrostatic

interactions in aqueous solutions typically improves their accuracy [66, 87, 88], but accounting for this dependence in models describing polymer-phase interactions is difficult, as there is little experimental data to provide information for how the relative permittivity of the sorbed water inside the polymer changes as a function of the external solution conditions.

With the knowledge that the Donnan – Manning – Born model describes ion sorption in the sulfonated polysulfones, the model can be used to understand the mechanisms driving previously unexplained structure/property relationships observed in the materials. For example, the Donnan – Manning – Born model provides an explanation for the observation that methoxy group incorporation did not influence the ion sorption properties in the polymers (Section 4.1.3). As discussed previously, the interactions described by the Manning and Born models have opposing effects on the thermodynamic non-ideality ions experience in the polymer matrix. For example, the self-interactions in the Born model cause thermodynamic non-ideality that deviates in the non-favorable direction while ion-polymer interactions described by the Manning model cause thermodynamic non-ideality that deviates in the favorable direction (Fig. 6). In polymers described by the Donnan – Manning – Born model, where both interactions are relevant, it follows that the changes in the polymer dielectric constant may cause changes in the ionic interactions that effectively cancel out (i.e., the more non-favorable Born interactions that suppress ion sorption are counteracted by the more favorable Manning interactions that promote ion sorption). This physical picture provides a potential explanation for the observation that suppressing the dielectric constant of the sulfonated polysulfones through methoxy group incorporation does not influence the polymer ion sorption properties.

In Nafion, the RMS log error for the Donnan – Manning – Born model improved relative to its value for that of the Donnan – Manning model (0.26 compared to 0.30, respectively) (Table 4), suggesting that dielectric exclusion may also influence ion sorption in Nafion. However, the magnitude of the improvement for Nafion was smaller than that for the sulfonated polysulfones, which decreased from 0.93 to 0.34 between the Donnan – Manning and Donnan – Manning – Born model, respectively (Table 4). These results suggest that it is less important to account for dielectric exclusion when modeling the ion sorption properties of Nafion relative to sulfonated polysulfones, which is consistent with a physical picture where in high dielectric constant polymers, primary ionic interactions (here, ion-polymer interactions described by the Manning model) govern ionic non-ideality, and secondary interactions (such as those between ions and polarization charges) are less relevant.

5. Conclusions

Both Donnan and dielectric exclusion mechanisms influenced the ion sorption properties of sulfonated polysulfones. Qualitatively, reducing the degree disulfonation of the sulfonated polysulfones, which increased the polymer fixed charge concentration, increased the Donnan exclusion. However, the incorporation of the polar methoxy group, which suppressed polymer dielectric constant, did not have a statistically significant influence on the dielectric exclusion mechanism. This result may be consistent with a physical picture where the suppression of polymer dielectric constant increased the extent of ionic non-ideality in both the favorable and non-favorable directions, and as a result, did not influence the overall polymer ion sorption properties.

The Donnan – Born, Donnan – Manning, and Donnan – Manning – Born models can be used to quantitatively describe ion sorption within the limits of the assumptions incorporated in the models. When applied to the sulfonated polysulfones, the Donnan – Born and Donnan – Manning models overpredict the deviation of the mean ionic activity coefficients (in the non-favorable and favorable directions, respectively) of the sulfonated polysulfones from ideality, and as a result did not provide quantitatively accurate predictions of the ion sorption coefficients. The Donnan – Manning – Born model, which accounted for

favorable interactions between ions and polymer as well as non-favorable interactions between ions and their induced polarization provided more accurate predictions of the ion sorption properties of sulfonated polysulfones. The Donnan – Manning – Born model also improved the accuracy of the predictions of the ion sorption properties of Nafion but to a much lesser extent than in sulfonate polysulfones. These results help provide explanations for the underlying mechanisms influencing the salt transport properties of hydrated charged polymers.

CRediT authorship contribution statement

Sean M. Bannon: Conceptualization, Formal analysis, Investigation, Methodology, Visualization, Writing – original draft, Writing – review & editing. **Geoffrey M. Geise:** Conceptualization, Funding acquisition, Project administration, Supervision, Writing – review & editing.

Declaration of competing interest

The authors declare that they have no known competing financial interests or personal relationships that could have appeared to influence the work reported in this paper.

Data availability

Data will be made available on request.

Acknowledgements

This material is based upon work supported, in part, by the National Science Foundation under Award No. CBET-1752048. Any opinions, findings and conclusions or recommendations expressed in this material are those of the authors and do not necessarily reflect the views of the National Science Foundation. Acknowledgement is made to the donors of the American Chemical Society Petroleum Research Fund for partial support of this research.

Appendix A. Supplementary data

Supplementary data to this article can be found online at <https://doi.org/10.1016/j.memsci.2023.122396>.

References

- [1] G.M. Geise, H.-S. Lee, D.J. Miller, B.D. Freeman, J.E. McGrath, D.R. Paul, Water purification by membranes: the role of polymer science, *J. Polym. Sci. B Polym. Phys.* 48 (2010) 1685–1718, <https://doi.org/10.1002/polb.22037>.
- [2] G.M. Geise, D.R. Paul, B.D. Freeman, Fundamental water and salt transport properties of polymeric materials, *Prog. Polym. Sci.* 39 (2014) 1–42, <https://doi.org/10.1016/j.progpolymsci.2013.07.001>.
- [3] M. Elimelech, W.A. Phillip, The future of Seawater desalination: energy, Technology, and the environment, *Science* 333 (2011) 712–717, <https://doi.org/10.1126/science.1200488>.
- [4] R.W. Baker, *Membrane Technology and Applications*, third ed., John Wiley & Sons, Chichester, West Sussex ; Hoboken, 2012.
- [5] W. Pusch, Chapter 1.4 Measurement techniques of transport through membranes, *Desalination* 59 (1986) 105–198, [https://doi.org/10.1016/0011-9164\(86\)90028-7](https://doi.org/10.1016/0011-9164(86)90028-7).
- [6] J.G. Wijmans, R.W. Baker, The solution-diffusion model: a review, *J. Membr. Sci.* 107 (1995) 1–21, [https://doi.org/10.1016/0376-7388\(95\)00102-1](https://doi.org/10.1016/0376-7388(95)00102-1).
- [7] D. Paul, Reformulation of the solution-diffusion theory of reverse osmosis, *J. Membr. Sci.* 241 (2004) 371–386, <https://doi.org/10.1016/j.memsci.2004.05.026>.
- [8] V.H. Hegde, M.F. Doherty, T.M. Squires, A two-phase model that unifies and extends the classical models of membrane transport, *Science* 377 (2022) 186–191, <https://doi.org/10.1126/science.abm7192>.
- [9] J. Kucera, Biofouling of Polyamide membranes: fouling mechanisms, Current Mitigation and Cleaning strategies, and future Prospects, *Membranes* 9 (2019) 111, <https://doi.org/10.3390/membranes9090111>.
- [10] Q. She, R. Wang, A.G. Fane, C.Y. Tang, Membrane fouling in osmotically driven membrane processes: a review, *J. Membr. Sci.* 499 (2016) 201–233, <https://doi.org/10.1016/j.memsci.2015.10.040>.

[11] H.B. Park, B.D. Freeman, Z.-B. Zhang, M. Sankir, J.E. McGrath, Highly chlorine-Tolerant polymers for desalination, *Angew. Chem. Int. Ed.* 47 (2008) 6019–6024, <https://doi.org/10.1002/anie.200800454>.

[12] A.E. Allegrezza, B.S. Parekh, P.L. Parise, E.J. Swiniarski, J.L. White, Chlorine resistant polysulfone reverse osmosis modules, *Desalination* 64 (1987) 285–304, [https://doi.org/10.1016/0011-9164\(87\)90103-2](https://doi.org/10.1016/0011-9164(87)90103-2).

[13] M. Stolov, V. Freger, Degradation of Polyamide membranes Exposed to chlorine: an Impedance spectroscopy Study, *Environ. Sci. Technol.* 53 (2019) 2618–2625, <https://doi.org/10.1021/acs.est.8b04790>.

[14] J. Kamcev, B.D. Freeman, Charged polymer membranes for Environmental/energy applications, *Annu. Rev. Chem. Biomol. Eng.* 7 (2016) 111–133, <https://doi.org/10.1146/annurev-chembiomeng-080615-033533>.

[15] J. Ran, L. Wu, Y. He, Z. Yang, Y. Wang, C. Jiang, L. Ge, E. Bakangura, T. Xu, Ion exchange membranes: New developments and applications, *J. Membr. Sci.* 522 (2017) 267–291, <https://doi.org/10.1016/j.memsci.2016.09.033>.

[16] T. Luo, S. Abdu, M. Wessling, Selectivity of ion exchange membranes: a review, *J. Membr. Sci.* 555 (2018) 429–454, <https://doi.org/10.1016/j.memsci.2018.03.051>.

[17] F.G. Donnan, The theory of membrane Equilibria, *Chem. Rev.* 1 (1924) 73–90, <https://doi.org/10.1021/cr60001a003>.

[18] S. Sarkar, A.K. SenGupta, P. Prakash, The Donnan membrane principle: Opportunities for Sustainable engineered processes and materials, *Environ. Sci. Technol.* 44 (2010) 1161–1166, <https://doi.org/10.1021/es9024029>.

[19] P. Aydogan Gokturk, R. Sujanani, J. Qian, Y. Wang, L.E. Katz, B.D. Freeman, E. J. Crumlin, The Donnan potential revealed, *Nat. Commun.* 13 (2022) 5880, <https://doi.org/10.1038/s41467-022-33592-3>.

[20] G.M. Geise, L.P. Falcon, B.D. Freeman, D.R. Paul, Sodium chloride sorption in sulfonated polymers for membrane applications, *J. Membr. Sci.* 423–424 (2012) 195–208, <https://doi.org/10.1016/j.memsci.2012.08.014>.

[21] F. Helfferrich, *Ion Exchange*, McGraw-Hill, New York, 1962.

[22] V. Freger, Ion partitioning and permeation in charged low-T* membranes, *Adv. Colloid Interface Sci.* 277 (2020) 102107, <https://doi.org/10.1016/j.cis.2020.102107>.

[23] M. Galizia, G.S. Manning, D.R. Paul, B.D. Freeman, Ion partitioning between brines and ion exchange polymers, *Polymer* 165 (2019) 91–100, <https://doi.org/10.1016/j.polymer.2019.01.026>.

[24] The Donnan law and its application to ion exchanger polymers, *Proc. R. Soc. Lond. A* 268 (1962) 339–349, <https://doi.org/10.1098/rspa.1962.0145>.

[25] G.E. Boyd, K. Bunzl, The Donnan equilibrium in cross-linked polystyrene cation and anion Exchangers, *J. Am. Chem. Soc.* 89 (1967) 1776–1780, <https://doi.org/10.1021/ja00984a003>.

[26] J. Kamcev, M. Galizia, F.M. Benedetti, E.-S. Jang, D.R. Paul, B.D. Freeman, G. S. Manning, Partitioning of mobile ions between ion exchange polymers and aqueous salt solutions: importance of counter-ion condensation, *Phys. Chem. Chem. Phys.* 18 (2016) 6021–6031, <https://doi.org/10.1039/C5CP06747B>.

[27] R. Sujanani, L.E. Katz, D.R. Paul, B.D. Freeman, Aqueous ion partitioning in Nafion: Applicability of Manning's counter-ion condensation theory, *J. Membr. Sci.* 638 (2021) 119687, <https://doi.org/10.1016/j.memsci.2021.119687>.

[28] N. Yan, D.R. Paul, B.D. Freeman, Water and ion sorption in a series of cross-linked AMPS/PEGDA hydrogel membranes, *Polymer* 146 (2018) 196–208, <https://doi.org/10.1016/j.polymer.2018.05.021>.

[29] D. Kitto, J. Kamcev, Manning condensation in ion exchange membranes: a review on ion partitioning and diffusion models, *J. Polym. Sci.* (2022) 20210810, <https://doi.org/10.1002/pol.20210810>.

[30] R.S. Kingsbury, O. Coronell, Modeling and validation of concentration dependence of ion exchange membrane permselectivity: Significance of convection and Manning's counter-ion condensation theory, *J. Membr. Sci.* (2020) 118411, <https://doi.org/10.1016/j.memsci.2020.118411>.

[31] G.S. Manning, Limiting laws and counterion condensation in polyelectrolyte solutions I. Colligative properties, *J. Chem. Phys.* 51 (1969) 924–933, <https://doi.org/10.1063/1.1672157>.

[32] J. Kamcev, D.R. Paul, B.D. Freeman, Ion activity coefficients in ion exchange polymers: Applicability of Manning's counterion condensation theory, *Macromolecules* 48 (2015) 8011–8024, <https://doi.org/10.1021/acs.macromol.5b01654>.

[33] K.S. Pitzer, J.M. Simonson, Thermodynamics of multicomponent, miscible, ionic systems: theory and equations, *J. Phys. Chem.* 90 (1986) 3005–3009, <https://doi.org/10.1021/j100404a042>.

[34] K.S. Pitzer, *Activity Coefficients in Electrolyte Solutions*, second ed., CRC Press, Boca Raton, 1991.

[35] R. Sujanani, O. Nordness, A. Miranda, L.E. Katz, J.F. Brennecke, B.D. Freeman, Accounting for ion Pairing effects on sulfate salt sorption in cation exchange membranes, *J. Phys. Chem. B* 127 (2023) 1842–1855, <https://doi.org/10.1021/acs.jpcb.2c07900>.

[36] Y.S. Oren, O. Nir, V. Freger, Analyzing ion uptake in ion-exchange membranes using ion association model, *J. Membr. Sci.* 690 (2024) 122202, <https://doi.org/10.1016/j.memsci.2023.122202>.

[37] K. Chang, H. Luo, S.M. Bannon, S.Y. Lin, W.-A.S. Agata, G.M. Geise, Methoxy groups increase water and decrease salt permeability properties of sulfonated polysulfone desalination membranes, *J. Membr. Sci.* 630 (2021) 119298, <https://doi.org/10.1016/j.memsci.2021.119298>.

[38] H. Luo, J. Aboki, Y. Ji, R. Guo, G.M. Geise, Water and salt transport properties of Triptycene-containing sulfonated polysulfone materials for desalination membrane applications, *ACS Appl. Mater. Interfaces* 10 (2018) 4102–4112, <https://doi.org/10.1021/acsami.7b17225>.

[39] C.H. Lee, B.D. McCloskey, J. Cook, O. Lane, W. Xie, B.D. Freeman, Y.M. Lee, J. E. McGrath, Disulfonated poly(arylene ether sulfone) random copolymer thin film composite membrane fabricated using a benign solvent for reverse osmosis applications, *J. Membr. Sci.* 389 (2012) 363–371, <https://doi.org/10.1016/j.memsci.2011.11.001>.

[40] B.J. Sundell, E.-S. Jang, J.R. Cook, B.D. Freeman, J.S. Riffle, J.E. McGrath, Cross-Linked disulfonated poly(arylene ether sulfone) Telechelic Oligomers. 2. Elevated transport performance with increasing Hydrophilicity, *Ind. Eng. Chem. Res.* 55 (2016) 1419–1426, <https://doi.org/10.1021/acs.iecr.5b04050>.

[41] W. Xie, G.M. Geise, B.D. Freeman, C.H. Lee, J.E. McGrath, Influence of processing history on water and salt transport properties of disulfonated polysulfone random copolymers, *Polymer* 53 (2012) 1581–1592, <https://doi.org/10.1016/j.polymer.2012.01.046>.

[42] M. Paul, H.B. Park, B.D. Freeman, A. Roy, J.E. McGrath, J.S. Riffle, Synthesis and crosslinking of partially disulfonated poly(arylene ether sulfone) random copolymers as candidates for chlorine resistant reverse osmosis membranes, *Polymer* 49 (2008) 2243–2252, <https://doi.org/10.1016/j.polymer.2008.02.039>.

[43] S.R. Choudhury, O. Lane, D. Kazerooni, G.S. Narang, E.S. Jang, B.D. Freeman, J. J. Lesko, J.S. Riffle, Synthesis and characterization of post-sulfonated poly(arylene ether sulfone) membranes for potential applications in water desalination, *Polymer* 177 (2019) 250–261, <https://doi.org/10.1016/j.polymer.2019.05.075>.

[44] A. Daryaei, G.C. Miller, J. Willey, S. Roy Choudhury, B. Vondrasek, D. Kazerooni, M.R. Burtner, C. Mittelstaedt, J.J. Lesko, J.S. Riffle, J.E. McGrath, Synthesis and membrane properties of sulfonated poly(arylene ether sulfone) statistical copolymers for Electrolysis of water: influence of Meta- and Para-Substituted Comonomers, *ACS Appl. Mater. Interfaces* 9 (2017) 20067–20075, <https://doi.org/10.1021/acsami.7b02401>.

[45] W. Xie, J. Cook, H.B. Park, B.D. Freeman, C.H. Lee, J.E. McGrath, Fundamental salt and water transport properties in directly copolymerized disulfonated poly(arylene ether sulfone) random copolymers, *Polymer* 52 (2011) 2032–2043, <https://doi.org/10.1016/j.polymer.2011.02.006>.

[46] K. Chang, H. Luo, G.M. Geise, Water content, relative permittivity, and ion sorption properties of polymers for membrane desalination, *J. Membr. Sci.* 574 (2019) 24–32, <https://doi.org/10.1016/j.memsci.2018.12.048>.

[47] M. Stolov, V. Freger, Membrane charge Weakly affects ion transport in reverse osmosis, *Environ. Sci. Technol. Lett.* 7 (2020) 440–445, <https://doi.org/10.1021/acs.estlett.0c00291>.

[48] H. Zhang, G.M. Geise, Modeling the water permeability and water/salt selectivity tradeoff in polymer membranes, *J. Membr. Sci.* 520 (2016) 790–800, <https://doi.org/10.1016/j.memsci.2016.08.035>.

[49] A. Yaroshchuk, M.L. Bruening, E. Zholkovskiy, Modelling nanofiltration of electrolyte solutions, *Adv. Colloid Interface Sci.* 268 (2019) 39–63, <https://doi.org/10.1016/j.cis.2019.03.004>.

[50] S. Bandini, D. Vezzani, Nanofiltration modeling: the role of dielectric exclusion in membrane characterization, *Chem. Eng. Sci.* 58 (2003) 3303–3326, [https://doi.org/10.1016/S0009-2509\(03\)00212-4](https://doi.org/10.1016/S0009-2509(03)00212-4).

[51] A. Parsegian, Energy of an ion crossing a low dielectric membrane: solutions to Four relevant electrostatic Problems, *Nature* 221 (1969) 844–846, <https://doi.org/10.1038/221844a0>.

[52] A.E. Yaroshchuk, Dielectric exclusion of ions from membranes, *Adv. Colloid Interface Sci.* 85 (2000) 193–230, [https://doi.org/10.1016/S0001-8686\(99\)00021-4](https://doi.org/10.1016/S0001-8686(99)00021-4).

[53] V. Freger, Dielectric exclusion, an éminence grise, *Adv. Colloid Interface Sci.* 319 (2023) 102972, <https://doi.org/10.1016/j.cis.2023.102972>.

[54] M. Born, *Volumen und Hydratationswärme der Ionen*, *Z. Physik.* 1 (1920) 45–48.

[55] K. Chang, G.M. Geise, Dielectric permittivity properties of hydrated polymers: measurement and connection to ion transport properties, *Ind. Eng. Chem. Res.* 59 (2020) 5205–5217, <https://doi.org/10.1021/acs.iecr.9b03950>.

[56] K. Chang, H. Luo, Influence of salt concentration on hydrated polymer relative permittivity and state of water properties, *Macromolecules* 54 (2021) 637–646, <https://doi.org/10.1021/acs.macromol.0c02188>.

[57] Z. Lu, G. Polizos, D.D. Macdonald, E. Manias, State of water in Perfluorosulfonic ionomer (Nafion 117) proton exchange membranes, *J. Electrochem. Soc.* 155 (2008) 10, <https://doi.org/10.1149/1.2815444>.

[58] A. Yaroshchuk, Non-steric mechanisms of nanofiltration: superposition of Donnan and dielectric exclusion, *Separation and Purification Technology* 22–23 (2001) 143–158, [https://doi.org/10.1016/S1383-5866\(00\)00159-3](https://doi.org/10.1016/S1383-5866(00)00159-3).

[59] Y. Ji, H. Luo, G.M. Geise, Specific co-ion sorption and diffusion properties influence membrane permselectivity, *J. Membr. Sci.* 563 (2018) 492–504, <https://doi.org/10.1016/j.memsci.2018.06.010>.

[60] Y. Yu, N. Yan, B.D. Freeman, C.-C. Chen, Mobile ion partitioning in ion exchange membranes immersed in saline solutions, *J. Membr. Sci.* 620 (2021) 118760, <https://doi.org/10.1016/j.memsci.2020.118760>.

[61] Y. Yu, Y. Li, N. Hossain, C.-C. Chen, Nonrandom two-liquid activity coefficient model for aqueous polyelectrolyte solutions, *Fluid Phase Equil.* 497 (2019) 1–9, <https://doi.org/10.1016/j.fluid.2019.05.009>.

[62] N. Lakshminarayanaiah, *Transport Phenomena in Membranes*, Academic Press, London, 1972.

[63] H.K. Gallage Dona, T. Olaiyiwola, L.A. Briceno-Mena, C.G. Arges, R. Kumar, J. A. Romagnoli, Determining ion activity coefficients in ion-exchange membranes with Machine Learning and molecular Dynamics Simulations, *Ind. Eng. Chem. Res.* 62 (2023) 9533–9548, <https://doi.org/10.1021/acs.iecr.3c00636>.

[64] P.W. Atkins, J. De Paula, *Atkins' Physical Chemistry*, tenth ed., Oxford University Press, Oxford, New York, 2014.

[65] P. Debye, E. Hückel, The theory of electrolytes. I. Freezing point depression and related phenomena', *Phys. Z.* (1923) 185–206.

[66] G.M. Kontogeorgis, B. Maribo-Mogensen, K. Thomsen, The Debye-Hückel theory and its importance in modeling electrolyte solutions, *Fluid Phase Equil.* 462 (2018) 130–152, <https://doi.org/10.1016/j.fluid.2018.01.004>.

[67] M.L. Michelsen, J.M. Mollerup, *Thermodynamic models : fundamentals & computational aspects*, in: *Tie-Line Productions*, first ed., 2004. Holte, Denmark.

[68] M.J. Braus, The Theory of Electrolytes. I. Freezing Point Depression and Related Phenomena (Translation), 2019. <https://minds.wisconsin.edu/handle/1793/79225>. (Accessed 25 September 2023).

[69] W. Xie, H. Ju, G.M. Geise, B.D. Freeman, J.I. Mardel, A.J. Hill, J.E. McGrath, Effect of free volume on water and salt transport properties in directly copolymerized disulfonated poly(arylene ether sulfone) random copolymers, *Macromolecules* 44 (2011) 4428–4438, <https://doi.org/10.1021/ma102745s>.

[70] J. Rumble, *CRC Handbook of Chemistry*, 98th ed., CRC Press LLC, Boca Raton, 2017.

[71] J. Kamcev, C.M. Doherty, K.P. Lopez, A.J. Hill, D.R. Paul, B.D. Freeman, Effect of fixed charge group concentration on salt permeability and diffusion coefficients in ion exchange membranes, *J. Membr. Sci.* 566 (2018) 307–316, <https://doi.org/10.1016/j.memsci.2018.08.053>.

[72] B.W. Rowe, B.D. Freeman, D.R. Paul, Effect of sorbed water and temperature on the Optical properties and density of thin Glassy polymer films on a Silicon Substrate, *Macromolecules* 40 (2007) 2806–2813, <https://doi.org/10.1021/ma0627931>.

[73] S.J. Paddison, G. Bender, K.-D. Kreuer, N. Nicoloso, T.A.Z. Jr, The microwave region of the dielectric spectrum of hydrated Nafion® and other sulfonated membranes, *J. N. Mater. Electrochem. Syst.* (2000) 293–302.

[74] Z. Lu, M. Lanagan, E. Manias, D.D. Macdonald, Two-port transmission line technique for dielectric property characterization of polymer electrolyte membranes, *J. Phys. Chem. B* 113 (2009) 13551–13559, <https://doi.org/10.1021/jp9057115>.

[75] H. Yasuda, C.E. Lamaze, L.D. Ikenberry, Permeability of solutes through hydrated polymer membranes. Part I. Diffusion of sodium chloride, *Makromol. Chem.* 118 (1968) 19–35, <https://doi.org/10.1002/macp.1968.021180102>.

[76] J. Kamcev, E.-S. Jang, N. Yan, D.R. Paul, B.D. Freeman, Effect of ambient carbon dioxide on salt permeability and sorption measurements in ion-exchange membranes, *J. Membr. Sci.* 479 (2015) 55–66, <https://doi.org/10.1016/j.memsci.2014.12.031>.

[77] K.M. Beers, D.T. Hallinan, X. Wang, J.A. Pople, N.P. Balsara, Counterion condensation in Nafion, *Macromolecules* 44 (2011) 8866–8870, <https://doi.org/10.1021/ma2015084>.

[78] G.M. Geise, B.D. Freeman, D.R. Paul, Sodium chloride diffusion in sulfonated polymers for membrane applications, *J. Membr. Sci.* 427 (2013) 186–196, <https://doi.org/10.1016/j.memsci.2012.09.029>.

[79] D.H. Gadani, V.A. Rana, S.P. Bhatnagar, A.N. Prajapati, A.D. Vyas, Effect of salinity on the dielectric properties of water, *Indian J. Pure Appl. Phys.* 50 (2012) 405–410.

[80] J. Wang, D.S. Dlamini, A.K. Mishra, M.T.M. Pendergast, M.C.Y. Wong, B.B. Mamba, V. Freger, A.R.D. Verliefde, E.M.V. Hoek, A critical review of transport through osmotic membranes, *J. Membr. Sci.* 454 (2014) 516–537, <https://doi.org/10.1016/j.memsci.2013.12.034>.

[81] C. Wang, S.J. Paddison, Mesoscale modeling of hydrated morphologies of sulfonated polysulfone ionomers, *Soft Matter* 10 (2014) 819–830, <https://doi.org/10.1039/C3SM52330F>.

[82] C.C. de Araujo, K.D. Kreuer, M. Schuster, G. Portale, H. Mendil-Jakani, G. Gebel, J. Maier, Poly(p-phenylene sulfone)s with high ion exchange capacity: ionomers with unique microstructural and transport features, *Phys. Chem. Chem. Phys.* 11 (2009) 3305, <https://doi.org/10.1039/b822069g>.

[83] K.D. Kreuer, On the development of proton conducting polymer membranes for hydrogen and methanol fuel cells, *J. Membr. Sci.* 185 (2001) 29–39, [https://doi.org/10.1016/S0376-7388\(00\)00632-3](https://doi.org/10.1016/S0376-7388(00)00632-3).

[84] D. Nguyen, J.-S. Kim, M.D. Guiver, A. Eisenberg, Clustering in carboxylated polysulfone ionomers: a characterization by dynamic mechanical and small-angle X-ray scattering methods, *J. Polym. Sci. B Polym. Phys.* 37 (1999) 3226–3232, [https://doi.org/10.1002/\(SICI\)1099-0488\(19991115\)37:22<3226::AID-POLB7>3.0.CO;2-M](https://doi.org/10.1002/(SICI)1099-0488(19991115)37:22<3226::AID-POLB7>3.0.CO;2-M).

[85] D.J. Yarusso, S.L. Cooper, Analysis of SAXS data from ionomer systems, *Polymer* 26 (1985) 371–378, [https://doi.org/10.1016/0032-3861\(85\)90196-X](https://doi.org/10.1016/0032-3861(85)90196-X).

[86] B. Vondrasek, C. Wen, S. Cheng, J.S. Riffle, J.J. Lesko, Hydration, ion distribution, and ionic network formation in sulfonated poly(arylene ether sulfones), *Macromolecules* 54 (2021) 302–315, <https://doi.org/10.1021/acs.macromol.0c01855>.

[87] G.M. Silva, X. Liang, G.M. Kontogeorgis, How to account for the concentration dependency of relative permittivity in the Debye-Hückel and Born equations, *Fluid Phase Equil.* 566 (2023) 113671, <https://doi.org/10.1016/j.fluid.2022.113671>.

[88] I.Yu Shilov, A.K. Lyashchenko, The role of concentration dependent static permittivity of electrolyte solutions in the Debye-Hückel theory, *J. Phys. Chem. B* 119 (2015) 10087–10095, <https://doi.org/10.1021/acs.jpcb.5b04555>.